available at www.sciencedirect.com

ScienceDirect

journal homepage: www.elsevier.com/locate/biochempharm

Modulation of hepatic microsomal triglyceride transfer protein (MTP) induced by S-nitroso-N-acetylcysteine in ob/ob mice

Claudia P.M.S. Oliveira [a,*], *Venâncio A.F. Alves* [b], *Vicência M.R. Lima* [a], *José Tadeu Stefano* [a], *Victor Debbas* [c], *Sandra Valéria Sá* [d], *Alda Wakamatsu* [b], *Maria Lúcia Corrêa-Giannella* [d], *Evandro Sobroza de Mello* [b], *Sofia Havaki* [e], *Dina G. Tiniakos* [e], *Evangelos Marinos* [e], *Marcelo G. de Oliveira* [f], *Daniel Giannella-Neto* [d], *Francisco R. Laurindo* [c], *Stephen Caldwell* [g], *Flair J. Carrilho* [a]

[a] *Department of Gastroenterology, University of São Paulo School of Medicine, Brazil*
[b] *Department of Pathology, University of São Paulo School of Medicine, Brazil*
[c] *Heart Institute, University of São Paulo School of Medicine, Brazil*
[d] *Laboratory for Cellular and Molecular Endocrinology (LIM-25), University of São Paulo School of Medicine, Brazil*
[e] *Laboratory of Histology and Embryology Medical School, National and Kapodistrian University of Athens, Greece*
[f] *Chemistry Institute, State University of Campinas, Brazil*
[g] *Department of Gastroenterology and Hepatology, University of Virginia, Charlottesville, VA, USA*

ARTICLE INFO

Article history:
Received 12 February 2007
Accepted 9 April 2007

Keywords:
NAFLD
NASH
MCD diet
MTP
S-Nitroso-N-acetylcysteine
SNAC

ABSTRACT

We evaluated the effects of a potent NO donor, S-nitroso-N-acetylcysteine (SNAC), on microsomal triglyceride transfer protein (MTP) expression in ob/ob mice. NAFLD was induced in male ob/ob mice using a methionine–choline deficient diet (MCD) concomitantly with oral SNAC fed solution ($n = 5$) or vehicle (control; $n = 5$) by gavage daily for 4 weeks. Livers were collected for histology and for assessing MTP by RT-qPCR, Western blot, immunohistochemistry and immunogold electron microscopy analyses. Histological analysis showed diffuse macro and microvesicular steatosis, moderate hepatocellular ballooning and moderate inflammatory infiltrate in ob/ob mice fed the MCD diet. With SNAC, mice showed a marked reduction in liver steatosis ($p < 0.01$), in parenchymal inflammation ($p = 0.02$) and in MTP protein immunoexpression in zone III ($p = 0.05$). Moreover, SNAC caused reduction of MTP protein in Western blot analysis ($p < 0.05$). In contrast, MTP mRNA content was significantly higher ($p < 0.05$) in mice receiving SNAC. Immuno-electron microscopy showed MTP localized in the rough endoplasmic reticulum of hepatocytes in both treated and untreated groups. However with SNAC treatment, MTP was also observed surrounding fat globules. Histological improvement mediated by a nitric oxide donor is associated with significantly altered expression and distribution of MTP in this animal model of fatty liver disease. Further studies are in progress to examine possible mechanisms and to develop SNAC as a possible therapy for human fatty liver disease.

* *Corresponding author at*: Departamento de Gastroenterologia, Faculdade de Medicina da Universidade de São Paulo, Av. Dr. Arnaldo, 455, 3° andar, # 3117 Cep.: 01246903-São Paulo, Brazil. Tel.: +55 11 30696673; fax: +55 11 30697830.
E-mail address: cpm@usp.br (Claudia P.M.S. Oliveira).

Abbreviations: NAFLD, nonalcoholic fatty liver disease; NASH, nonalcoholic steatohepatitis; MCD, methionine–choline deficient diet; SNAC, S-Nitroso-N-acetylcysteine; MTP, microsomal triglyceride transfer protein

0006-2952/$ – see front matter © 2007 Elsevier Inc. All rights reserved.
doi:10.1016/j.bcp.2007.04.013

1. Introduction

Nonalcoholic steatohepatitis (NASH) is an important form of liver disease that may progress to cirrhosis and liver failure [1–3]. The mechanisms that mediate the transition from steatosis to NASH remain unknown. The 'two-hit' hypothesis has been proposed to explain the pathogenesis of NASH, with an initial metabolic disturbance causing steatosis and a second pathogenic stimulus promoting oxidative stress, increased generation of reactive oxygen species (ROS), lipid peroxidation, and resultant NASH [4–6]. Insulin resistance plays a major role in hepatic fat accumulation through increased influx of free fatty acids (FFA) from peripheral fat stores due to enhanced lipolysis, increased *de novo* hepatocyte triglyceride synthesis from glucose and reduced apoB production, which diminishes fat export from the liver [7,8].

Microsomal triglyceride transfer protein (MTP) has a pivotal role in lipoprotein assembly in the endoplasmic reticulum (ER). MTP is an ER resident protein that forms a heterodimer with protein disulfide isomerase (PDI) [9]. It is known that apoB inserted in the ER undergoes disulfide bond formation followed by association with triglycerides by the complex formed by PDI/MTP [10]. In addition, interaction of MTP with PDI likely stabilizes the alpha subunit of MTP, inducing its retention within the ER, through the PDI C-terminal sequence Lys-Asp-Glu-Leu (KDEL) [9]. It has been demonstrated that, *in vitro*, MTP mobilizes neutral lipids from donor vesicles to acceptor vesicles [11]. This lipid transfer activity of MTP appears to be essential for the lipidation of apoB and for its assembly in lipoproteins and secretion from the liver and intestine [12]. This claim is reinforced by the finding that defects in MTP lead to abetalipoproteinemia, an autosomal recessive disease characterized by exceedingly low levels of apoB-containing lipoproteins in the plasma [13]. In addition, pharmacological inhibitors of the transfer activity of MTP were shown to decrease apoB and triglyceride secretion by cells in culture, to block the production of VLDL (very low density lipoprotein) in rodents, and to normalize plasma lipoprotein levels in animal models, without increasing hepatic triglycerides [14]. Down-regulation of MTP gene expression facilitates intracellular fat accumulation in hepatocytes increasing the susceptibility to hepatic steatosis. These observations point to an inverse correlation between MTP expression and NAFLD development.

Previous studies have shown that treatment with *S*-nitroso-*N*-acetylcysteine (SNAC), a potent inhibitor of lipid peroxidation, prevented nonalcoholic fatty liver disease (NAFLD) induced by a choline deficient diet in rats [15] and promoted down-regulation of several genes linked to fatty acid metabolism [16].The aim of this study was to further investigate the effect of oral administration of SNAC in the prevention of NASH in ob/ob mice fed a methionine–choline deficient diet and to correlate this effect with MTP expression. While no animal model perfectly replicates human NASH, this two hit model including leptin deficiency which produces steatosis and choline deficiency which provokes cell injury (including hepatocyte ballooning and inflammation) offers a reliable model for investigating potential forms of therapy.

2. Materials and methods

2.1. SNAC synthesis

SNAC was synthesized through the *S*-nitrosation of *N*-acetyl-L-cysteine (Sigma Chemical, St. Louis, MO) in an acidified sodium nitrite solution [17]. Stock SNAC solutions were further diluted in PBS. Solutions were diluted to 2.4×10^{-4} mol/L in PBS (pH 7.4) before administration. All the experiments were carried out using analytical grade water from a Millipore Milli-Q Gradient filtration system.

2.2. Animals

Male ob/ob mice (Jackson Laboratories, Bar Harbor, Maine, USA), weighing 30–40 g, were housed in temperature and humidity controlled rooms, kept in a 12-h light/dark cycle and provided unrestricted amounts of food and water. All procedures for animal experimentation were in accordance to the Helsinki Declaration of 1975 (*NIH Publication No. 85-23, revised 1996*) and the Guidelines of Animal Experimentation from the University of São Paulo School of Medicine. NASH was induced in the ob/ob mice by methionine/choline deficient (MCD) diet (62.5% carbohydrate with starch and sucrose; 17% protein with casein without methionine–choline; 7% lipid with soybean oil; 1% AIN-93M vitamin mix; 3.5% AIN-93M mineral mix [Rhoster Ind. Com. Ltd., SP, Brazil]) for 4 weeks. NASH was defined in this animal model by the presence of both macro- and microvesicular steatosis, hepatocellular ballooning, as well as a mixed lobular inflammatory infiltrate in zone III.

Ob/ob mice were randomly assigned to receive oral SNAC solution (1.4 μmol/kg) ($n = 5$) (MCD + SNAC group) or vehicle (physiologic Ringer's) ($n = 5$) (MCD group) both by gavage, daily. Ob/ob mice with standard diet were used as controls (Control group). After 4 weeks of treatment with SNAC or vehicle associated with MDC diet, ob/ob mice were sacrificed and samples of liver tissue were taken for histopathological analysis. RT-qPCR for mRNA MTP content and Western blot for 97-kDa murine MTP protein were performed in all liver samples as described below.

2.3. Laboratory evaluation

Serum alanine amininotransferase (ALT), aspartate aminotransferase (AST), cholesterol and triglycerides levels were analyzed by standard methods using automated techniques.

2.4. Histopathology and immunohistochemistry analyses

Fragments of liver tissues were fixed in formaldehyde saline (4%) and processed for hematoxylin–eosin (HE) and Masson Trichrome stains. Histological markers of NAFLD activity (steatosis 0–3, ballooning 0–2 and lobular inflammation 0–3) were assessed according to Histological Scoring System for Nonalcoholic Fatty Liver Disease (NASH Activity Score or NAS), recently published by the Pathology Committee of the NASH Clinical Research Network [18].

2.5. Immunohistochemical detection of MTP

After treatment of tissue sections with 3%, H_2O_2, antigen retrieval was achieved by incubation with a sodium citrate solution, pH 6.0 for 40 min in a steamer. MTP primary antibody was a rabbit nonspecific polyclonal IgG anti-MTP (Bristol-Myers-Squibb, USA), at a dilution 1:200. Incubation for 30 min at 37 °C was followed by additional 16 h (overnight) at 4 °C. Signal amplification was achieved through non-biotin method ENVISION-PLUS [DAKOCytomation, USA (cod. K4003)] for 30 min at 37 °C. Signal development was provided by a solution with 3,3-diaminobenzidine tetrahydrochloride (DAB) (Sigma Chemical Co., USA) and 0.01% H_2O_2. Positive and negative controls were performed in the same batch. MTP immunoexpression was semi-quantitated in hepatocytes from each acinar zone as follows: 0 = negative; 1+ = staining of less than 5% of hepatocytes; 2+ = 5–25%; 3+ = > 25%.

2.6. Immuno-electron microscopy for the assessment of MTP

The ultrastructural distribution of MTP was studied, applying the immunogold method, in liver samples of two cases of SNAC-treated mice and in liver samples of two cases of mice without SNAC treatment. All samples were chosen randomly from the collected material of this study. LRWhite-resin thin sections (60–80 nm thick) were cut with a Diatome diamond knife on a Leica Ultracut R ultramicrotome and were collected onto 200 mesh Formvar-coated nickel grids. MTP immunogold labeling was carried out according to the method of Polak and Van Noorden [19], modified as described previously [20]. Incubations were carried out by floating the grids on drops of solutions at room temperature (RT), except for the primary antibody step. The multiwell Terasaki plates were used as humid chambers. Grids were first incubated for 4 min on drops of 0.05 M Tris/HCl buffer, pH 7.4, and then on blocking buffer [0.05 M Tris/HCl, pH 7.4 + 1% bovine serum albumin (BSA) + 0.1% coldwater fish gelatin + 5% normal goat serum (NGS) + 0.1% Tween-20] for 30 min. Grids were then incubated with primary rabbit polyclonal IgG anti-MTP (Bristol-Myers-Squibb, USA) diluted 1:10 and incubated in Terasaki plate overnight at 4 °C. Control sections were incubated in the absence of primary antibody. The grids were rinsed in 0.05 M Tris/HCl, pH 7.4 and washed in 0.05 M Tris/HCl, pH 7.4 containing 0.1% Tween-20 (solution I), then in 0.05 M Tris/HCl, pH 7.2 containing 0.4% BSA and 0.1% Tween-20 (solution II) and finally in 0.05 M Tris/HCl, pH 8.2 containing 2% BSA and 0.1% Tween-20 (solution III). The grids were incubated for 1 h at room temperature in the secondary colloidal gold antibody (goat anti-rabbit IgG conjugated to 15 nm gold particles), diluted 1:40 in solution III. Consequently, the grids were washed in solution II, solution I and distilled water. Finally, they were dried and counterstained with ethanolic uranyl acetate and lead citrate. Using a random digit table, sections were selected from the grid boxes and viewed in a Zeiss EM 900 at 80 kV accelerating voltage, with an objective aperture of 30 μm. By means of a calibrated motorized stage, fields were selected at random and electron micrographs were taken for the statistical evaluation of the immunogold labeling. The photomicrographs were recorded on Kodak Electron Image film SO-163 (gelatin plates, 8 cm × 10 cm, code no.: 1679257), which were subsequently developed with the Kodak D-19 developer. Electron micrographs were printed on a Xerox N2025 high resolution laser printer at 1200 dpi. For quantification, a special grid (with 25 squares) was applied on each sample photomicrograph and immunoreactive granules were counted. Number of granules per grid square, total number of granules and mean/photograph was noted for each case. The number of granules per grid square as well as the total number of granules and mean/photograph were noted in each case.

2.7. Liver RNA extraction

After liver tissue pulverization (~50 mg) with a dismembrator (B. Braun Biotech International, Melsungen, Germany) at liquid nitrogen temperature, total RNA was prepared using Trizol reagent (Invitrogen Life Technologies, Carlsbad, CA, USA) according to the manufacturer's recommendations. Total RNA was dissolved in RNase-free water and RNA concentration was determined spectrophotometrically. RNA integrity was judged appropriate at a 260/280 nm ratio >1.8 and without signs of degradation on agarose gel. Samples were kept at −80 °C until processing by reverse transcription-quantitative polymerase chain reaction (RT-qPCR) analyses.

2.8. RT-qPCR analyses

Transcript levels of MTP were determined by RT-qPCR and the results were normalized according to corresponding values of housekeeping β-actin mRNA. Gene-specific primer pairs were located on two adjacent exons to achieve a high level of specificity and to avoid detection of genomic DNA. Primers were designed to have similar GC contents and annealing temperatures using the Primer3 Program (http://frodo.wi.mit.edu/cgi-bin/primer3/primer3_www.cgi) [21]:

- β-Actin (165-bp product) [NM_007393]:
  - Sense: 5′-TGT TAC CAA CTG GGA CGA CA-3′
  - Antisense: 5′-GGG GTG TTG AAG GTC TCA AA-3′
- MTP (171-bp product) [NM_008642]:
  - Sense: 5′-CCT CTT GGC AGT GCT TTT TC-3′
  - Antisense: 5′-ATT TTG TAG CCC ACG CTG TC-3′

mRNA analyses expressions were carried out in a Rotor-Gene RG-3000 (Corbett Research, Sidney, Australia) using Quantitect SYBR Green RT-PCR for quantitative, real time, one step RT-PCR (Qiagen GmbH, Hilden, Germany), according to the instructions provided by the manufacturer. Reactions lacking reverse transcriptase were also run to generate controls for assessment of genomic DNA contamination. The reaction mixture consisted of 12.5 μL of SYBR RT-PCR Master Mix, 0.25 μL of QuantiTect RT Mix, 0.2 mM sense/antisense primers and 5 μL (20 ng/μL) of total RNA template. The reaction was incubated under the following cycling conditions: 50 °C for 30 min for RT, heating to 95 °C for 15 min, and then 35 cycles at 94 °C for 20 s, 56 °C for 30 s and 72 °C for 30 s. Fluorescence changes were monitored after each cycle, and melting curve analysis was performed at the end of cycles to verify PCR product identity (72 °C ramping to 99 °C at 0.2 °C/s with continuous fluorescence readings). Specificity

Table 1 – Levels of alanine amininotransferase (ALT), aspartate aminotransferase (AST), cholesterol and triglycerides in the serum of ob/ob mice fed with methionine–choline deficient diet (MCD) which received or not SNAC by gavage for 4 weeks (MCD + SNAC)

Group	N	AST (U/L)	ALT (U/L)	Triglycerides (mg/dL)	Cholesterol (mg/dL)	Weight change (%)
Control	6	146 ± 63	25 ± 2	75 ± 35	89 ± 31	+14.6*
MCD	6	624 ± 461	230 ± 165	93 ± 27	105 ± 49	+4.8
MCD + SNAC	6	193 ± 18δ	22 ± 13δ	62 ± 23	89 ± 44	−1.0

References values, AST: 10–34 mg/dL; ALT: 10–44 mg/dL. cholesterol and triglycerides: 45–89 mg/dL.
δ $p < 0.05$; MCD × MCD/SNAC
* $p < 0.05$; data expressed as mean ± S.D.

of amplicons was also ensured by agarose gel electrophoresis to visualize a unique product fragment of the appropriate size.

mRNA content of MTP was determined as the number of transcripts relative to those of β-actin and additionally normalized to the mean value of control liver (obtained from the Control group). To evaluate the amplification efficiency of each target and housekeeping genes, standard curves were constructed from a control liver RNA sample using duplicate serial dilutions with five different RNA concentrations (500, 100, 20, 4 and 0.8 ng/μL). To evaluate the relative expression ratio of MTP gene compared with β-actin and efficiency values of both set of primers, the mathematical model described by Pfaffl was used [22], once the amplification efficiency with control gene was different. Amplification of MTP and housekeeping control gene was done in duplicate from each sample.

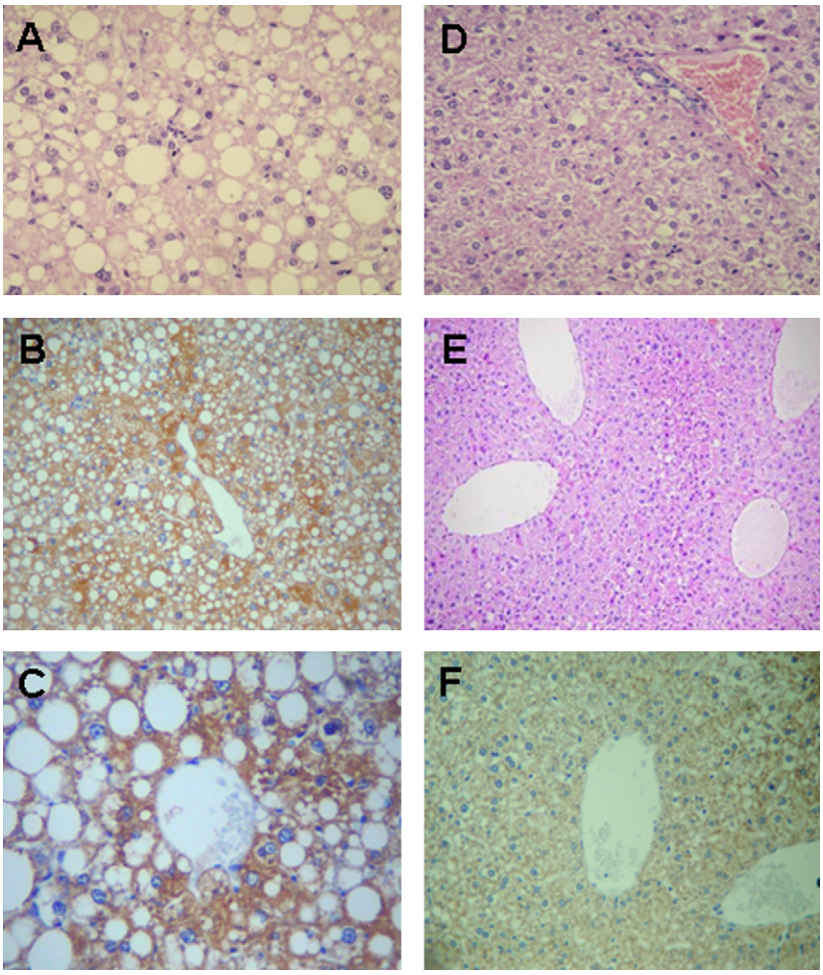

Fig. 1 – Morphological and Immunohistochemical features. MCD-fed mice without SNAC (MCD group): (A) steatohepatitis depicting steatosis grade 3 and lobular inflammation (HE, 200×); (B) MTP immunoexpression in innumerous hepatocytes (3+) (MTP, Envision, 100×); (C) strong MTP immunoexpression in zone 3 hepatocytes (MTP, Envision, 200×). MCD-fed mice treated with SNAC (MCD + SNAC): (D) portal and periportal areas without relevant histological lesions (HE, 100×); (E) centilobular areas almost devoid of steatosis (HE, 100×); (F) minimal MTP immunoexpression in zone 3 area (MTP, Envision, 100×).

Table 2 – Median of mRNA expression by RT-qPCR and immunoexpression by immunohistochemistry (IHQ) of MTP in the liver of ob/ob mice fed a methionine–choline deficient diet (MCD group) and which received oral SNAC solution by gavage for 4 weeks (MCD + SNAC group)

	N	MCD group	MCD + SNAC group	p value
MTP mRNA expression [median (min–max)] AU	5	1.10 (0.72–1.20)	1.66 (1.06–1.79)	0.007
MTP expression by lHQ [median (min–max)]	5	3.00 (2.00–3.00)	1.00 (1.00–3.00)	0.05

AU: arbitrary unit; IHQ: immunohistochemistry.

Inter-assay variation was investigated in two different experimental runs performed on different days.

2.9. Microsomal triglyceride transfer protein (MTP) Western blots

Livers from six mice were dissected, washed with ice-cold buffer (5 mM Tris, pH 7.4), and minced into pieces with a razor blade. The pieces were homogenized in ice-cold homogenization buffer (250 mM sucrose, 8 mM Tris, pH 7.4). The homogenate was centrifuged at 60 × g for 10 min. The supernatant fluid was removed and centrifuged again at 600 × *g*, 8,500 × *g* and 17,500 × *g* for 10 min each. The postmitochondrial supernatant fluid was removed and centrifuged at 105,000 × *g* for 90 min. The pellet, representing the microsomal vesicles, was resuspended in fresh lysis buffer (20 mM Hepes, 150 mM NaCl, 10% Glycerol, 1% Triton, 1 mM EDTA, 1.5 mM $MgCl_2$, 1 μg/mL aprotinin, 1 μg/mL leupeptin, 1 mM PMSF). The proteins were size-fractionated on a 10% polyacrylamide/SDS gel (30 μg of protein per lane); the separated proteins were then electrophoretically transferred to a nitrocellulose membrane. The Western blot was probed with a rabbit antiserum against MTP (Bristol-Myers Squibb, USA). The membranes were blocked in blocking buffer (TBS-T 0.1% supplemented with 5% nonfat milk) at room temperature for 2 h. After the primary antibody incubation (1:1000 dilution) overnight at 4 °C, the blots were washed with TBS-T 0.1% and incubated for 1 h with horseradish peroxidase-conjugated goat anti-rabbit IgG (Amersham Corp., Arlington Heights, USA). Bands were visualized using enhanced chemiluminescence (Amersham Corp., Arlington Heights, USA) and exposed to X-ray film.

2.10. Statistical analysis

Since most of the variables studied herein were semi-quantitative, non-parametric approach was provided for multiple comparison methods. For biochemical analysis, the results of the groups were compared using univariate analysis of variance. Regarding immuno-electron microscopy, since the granules were directly counted, an assessement of whether the distribution of the results was normal or not, Kolmogorov–Smirnov and Shapiro–Wilk tests were perfomed with values = 0.2000 and 0.528, respectively, thus showing a non-normal distribution. Among the non-parametric tests, we assessed our results to immuno-electron microscopy and Immunohistochemical by Mann–Whitney and by χ^2, with pretty similar results. Concerning RT-qPCR, since assumptions for a parametric test were not valid, data was evaluated by Wilcoxon Mann–Whitney Test for analyzing the overlap between distributions of two independent groups. The Mann–Whitney *U*-test was used to evaluate statistical significance of MTP Western blots expression among the groups. Statistical significance was set at p value <0.05.

3. Results

Biochemical analysis demonstrated that serum AST and ALT concentrations were highly elevated in the MCD group. SNAC treatment led to a marked decrease in the concentrations of ALT and AST. Nevertheless, cholesterol and triglycerides levels were unaltered with SNAC treatment (Table 1).

Histopathological analysis showed that ob/ob mice in the Control group (standard diet) there was only mild ballooning and minimal inflammation while in the MCD group ob/ob mice developed diffuse macro- and microvesicular steatosis, moderate hepatocellular ballooning and a moderate lobular mixed inflammatory infiltrate (Fig. 1A). As previously shown [16], MCD + SNAC group mice demonstrated a marked decrease in liver steatosis ($p < 0.01$) and in parenchymal inflammation ($p = 0.02$) (Fig. 1D and E). These results show that SNAC treatment can abolish the development of NAFLD in these animal models. We also observed strong MTP immunoexpression in zone 3 hepatocytes in the MCD group (Fig. 1B and C) which was reduced in zone 3 with SNAC therapy ($p = 0.05$) (Fig. 1F, Table 2). Similarly, the expression of hepatic MTP in microsomes evaluated by Western blot was reduced in SNAC-treated ob/ob mice ($p = 0.05$) (Fig. 2).

Ultrastructural examination showed that MTP-immunogold granules were localized to the rough ER membrane, as well as in its lumen in both groups (Fig. 3A). SNAC treatment promoted an alteration in the intracellular distribution of MTP as shown by the increased detection of MTP around the fat vesicles localized in ER (Fig. 3B). Quantitation of MTP immunoreactive granules in SNAC-treated samples showed

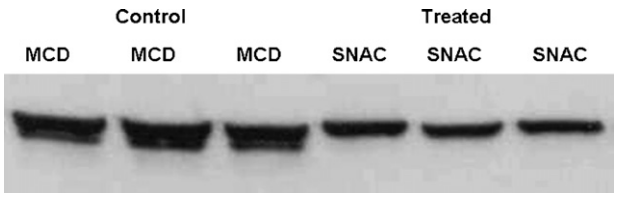

Fig. 2 – Hepatic microsomal triglyceride transfer protein (MTP) expression in MCD and MCD + SNAC groups. Microsomal protein was isolated from mouse livers and used for determination of triglyceride transfer protein expression by Western blot as described in methods. Bands were visualized using enhanced chemiluminescence (Amersham) and exposed to X-ray film. MTP expression was reduced in SNAC-treated ob/ob mice.

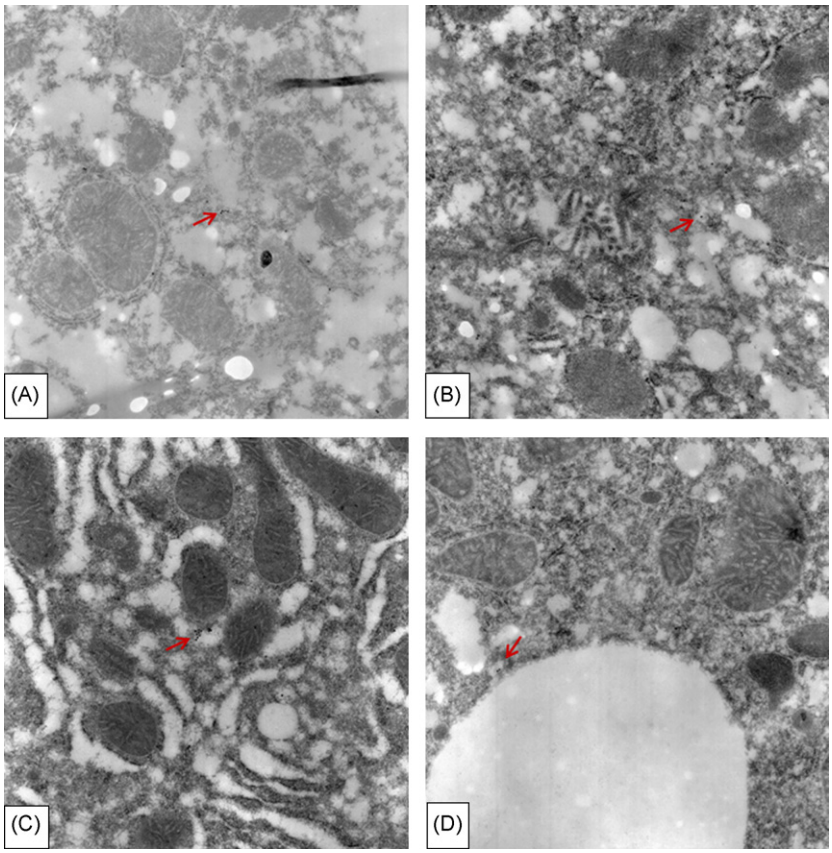

Fig. 3 – (A and B) MCD group: MTP immunogold localization on rough endoplasmic reticulum (RER) membrane and in its lumen (original magnification 20,000×). (C and D) MCD + SNAC group: MTP-immunoreactive granules are also observed in RER vesicles (arrow) (original magnification 20,000×).

no significant difference (0.5699 ± 0.2286) in comparison to non-treated animals (0.4533 ± 0.1887) ($p = 0.467$).

In contrast to the findings of protein expression, as shown Table 2, mRNA content of MTP was significantly higher ($p < 0.05$) in livers of SNAC-treated mice (1.46 ± 0.36) in comparison to the MCD group (1.00 ± 0.22).

4. Discussion

In the present study, we found that administration of SNAC was associated with reduction in histological criteria of experimental NASH concomitantly with reduction of MTP protein expression measured by both Western blot and immunohistochemistry, increase of MTP mRNA content and an alteration in the intracellular distribution of MTP.

A series of investigations in NAFLD have demonstrated several different rodent models that exhibit histological evidence of hepatic steatosis. Nevertheless, the features of true NASH that should include at least ballooning hepatocyte degeneration in addition to fatty change and an inflammatory infiltrate [18] have been less frequently demonstrated in these models [23]. One of the models that has been employed by many researchers is the genetic leptin-deficient (ob/ob) or leptin-resistant (db/db) mouse [23,24]. However, the limited fibrotic capacity of a leptin-deficient model [25] means that it is best suited to studies investigating the mechanisms behind the development of steatosis and the transition to NASH. Although ob/ob mice develop spontaneous liver steatosis, the development of a more significant injury requires the administration of a so-called "second metabolic hit" such as a MCD diet, a classical model of NAFLD, in which the animal develop steatosis, NASH and fibrosis [15,24]. In the present study, ob/ob mice receiving the MCD diet developed moderate diffuse macro- and microvesicular steatosis, hepatocellular ballooning, and a diffuse mixed lobular inflammatory infiltrate. The presence of cellular ballooning is characteristic of NASH although fibrosis was not observed because of the leptin deficiency.

The development of NASH in mice is dependent on the activation of pathways of hepatic lipid turnover, which are modulated by genes such as PPARs, ChREBP, SREBP1 and MTP which lipidates apolipoprotein B into triglyceride-rich VLDL particles [26–29]. Phillips et al. showed a significantly increased MTP mRNA in liver of obese rats and noted a correlation between MTP mRNA and MTP activity [30]. However, the relationship between expression of MTP mRNA and the activity or expression of MTP protein has not as yet been elucidated as exemplified by a report of dissociation between MTP mRNA levels and MTP activity [31]. These conflicting findings suggest that MTP mRNA might not strictly parallel MTP protein expression as our findings also suggest,

since we observed a reduction of MTP protein expression concomitantly with an increased mRNA content after SNAC treatment.

As it has been shown that inhibition of MTP activity in mice results in impaired hepatic lipoprotein secretion and steatosis [32] and, in the present study, the opposite effect was observed, it seems improbable that the decrease in MTP protein following SNAC treatment be a primary event, alternatively, it might occur secondary to other beneficial effects associated to SNAC, since it has been previously demonstrated that this NO donor elicits down-regulation of genes belonging to fatty acid biosynthesis pathways [16], possibly resulting in prevention of fatty accumulation.

We could also hypothesize that SNAC treatment induces a posttranslational modification of the MTP-PDI complex through a transnitrosation reaction with free sulfhydryl residues of the PDI, as demonstrated for other NO donors. Both, MTP and PDI possess free –SH moieties that can be nitrosated generating –SNO groups [33]. It remains to be elucidated if this posttranslational mechanism would explain the altered intracellular distribution of MTP observed by immuno-electronic microscopy after SNAC treatment. As lipidation of apoB can occur by two different pathways, i.e., through free MTP or through MTP associated with lipid vesicles and knowing that the latter pathway results in a faster assembly of apoB-containing lipoproteins [34–36], we speculate that the pattern of increased detection of MTP around the fat vesicles localized in ER could favor a more efficient apoB lipidation, contributing to prevention of NASH in this experimental model. However, SNAC treatment did not promote an augmentation in serum triglycerides and further studies using Triton injection are necessary to establish the final effect of MTP modulation on hepatic lipoprotein secretion.

Although the exact mechanism underlying the beneficial effect of SNAC is still unknown, the findings that this compound modulates MTP expression open new perspectives on the study of the effects of SNAC not only in the liver, but also in the small intestine, where MTP plays a pivotal role in lipid absorption. Further studies are underway to examine these questions and to develop SNAC as a possible therapy for NASH.

Acknowledgements

The authors acknowledge the Bristol Myers Squibb, USA and the supervision of statistical analyses by Dr Luiz Fernando Ferraz Silva. Fundação de Amparo à Pesquisa do Estado de São Paulo (FAPESP) and Alves de Queiroz Family Fund For Research.

REFERENCES

[1] Powell EE, Cooksley WG, Hanson R, Searle J, Halliday JW, Powell LW. The natural history of nonalcoholic steatohepatitis: a follow-up study of forty-two patients for up to 21years. Hepatology 1990;11:74–80.

[2] Falck-Ytter Y, Younossi ZM, Marchesini G, McCullough AJ. Clinical features and natural history of nonalcoholic steatosis syndromes. Semin Liver Dis 2001;21:17–26.

[3] Zafrani ES. Non-alcoholic fatty liver disease: an emerging pathological spectrum. Virchows Arch 2004;444:3–12.

[4] Day CP, James OFW. Steatohepatitis: a tale of two 'hits'? Gastroenterology 1998;114:842–5.

[5] McCullough AJ. Pathophysiology of nonalcoholic steatohepatitis. J Clin Gastroenterol 2006;40(Supp1):S17–29.

[6] Chitturi S, Farrell G. Ethiopathogenesis of nonalcoholic steatohepatitis. Semin Liver Dis 2001;21(1):27–41.

[7] Marchesini G, Brizi M, Morselli-Labate AM, Bianchi G, Bugianesi E, McCullough AJ, et al. Association of nonalcoholic fatty liver disease with insulin resistance. Am J Med 1999;107:450–5.

[8] Larter CZ, Farrell GC. Insulin resistance, adiponectin, cytokines in NASH: which is the best target to treat? J Hepatol 2006;44:253–61.

[9] Wetterau JR, Lin MCM, Jamil H. Microsomal triglyceride transfer protein. Biochem Biophys Acta 1997;1345:136–50.

[10] Lamberg A, Jauhiainen M, Metso J, Ehnholm C, Shoulders C, Scott J, et al. The role of protein disulphide isomerase in the microsomal triacylglycerol transfer protein does not reside in its isomerase activity. Biochem J 1996;315:533–6.

[11] Shelnea GS, Ingran MF, Huang XF, DeLozier. Apoliprotein B in the rough endoplasmatic reticulum: translation, translocation and the initiation of lipoprotein assembly. J Nutr 1999;129:456S–62S.

[12] Gordon DA, Wetterau JR, Greg RE. Microsomal triglyceride transfer protein: a protein complex required for the assembly of lipoprotein particles. Trends Cell Biol 1995;5:317–21.

[13] Shoulders CC, Brett DJ, Bayliss JD. Abetalipoproteinemia is caused by defects of the gene encoding the 97 kDa subunit of microsomal triglyceride transfer protein. Hum Mol Genet 1993;2(12):2109–16.

[14] Aggarwal D, West KL, Zern TL, Shrestha S, Vergara-Jimenez M, Fernandez ML. JTT-130, a microsomal triglyceride transfer protein (MTP) inhibitor lowers plasma triglycerides and LDL cholesterol concentrations without increasing hepatic triglycerides in guinea pigs. BMC Cardiovasc Dis 2005;5:30.

[15] Oliveira CPMS, Simplicio FI, Lima VMR, Yuahasi K, Lopasso FP, Alves VAF, et al. Oral administration of S-nitroso-N-acetylcysteine prevents the onset of non alcoholic fatty liver disease *n* rats. World J Gastroenterol 2006;12(12): 1905–11.

[16] Oliveira CPMS, Stefano JT, Lima VMR, Sa SV, Simplicio FI, Mello ES, et al. Hepatic gene expression profile associated with non-alcoholic steatohepatitis protection by S-nitroso-N-acetylcysteine in ob/ob mice. J Hepatol 2006;45:725–33.

[17] de Oliveira MG, Shishido SM, Seabra AB, Morgon NH. Thermal stability of primary S-nitrosothiols: roles of autocatalysis and structural effects on the rate of nitric oxide release. J Phys Chem 2002;106:8963–70.

[18] Kleiner DE, Brunt EM, Van Natta ML, Behling C, Contos MJ, Cummings OW, et al. Nonalcoholic Steatohepatitis Clinical Research Network. Design and validation of a histologic scoring system for NAFLD. Hepatology 2005;41:1313–21.

[19] Polak JM, Van Noorden S. Post-embedding immunocytochemistry for the transmission electron microscope. In: Polak JM, Van Noorden S, editors. Introduction to immunocytochemistry. Oxford: Bios Scientific Publishers; 1997. p. 81–9.

[20] Havaki S, Voloudakis-Baltatzis I, Goutas N, Arvanitis LD, Vassilaros SD, Arvanitis DL, et al. Nuclear localization of cytokeratin 8 and the O-linked *N*-acetylglucosamine containing epitope H in epithelial cells of infiltrating ductal breast carcinomas. A combination of immunogold and

EDTA regressive staining methods. Ultrastruct Pathol 2006;30:1–10.
[21] Rozen S, Skaletsky HJ. Primer3 on the WWW for general users and for biologist programmers. In: Krawetz S, Misener S, editors. Bioinformatics methods and protocols. Totowa: Humana Press; 2000. p. 365–86.
[22] Pfaffl MW. A new mathematical model for relative quantification in real time RT-PCR. Nucl Acids Res 2001;29:2002–7.
[23] Anstee QM, Goldin RD. Mouse models in non-alcoholic fatty liver disease and steatohepatitis research. Int J Exp Path 2006;87:1–16.
[24] Koteish A, Diehl AM. Animal models of steatosis. Semin Liver Dis 2001;21:89–104.
[25] Potter JJ, Rennie-Tankesley L, Mezey E. Influence of leptin in the development of hepatic fibrosis produced in mice by Schistosoma mansoni infection and by chronic carbon tetrachloride administration. J Hepatol 2003;38(3):281–8.
[26] Inoue M, Ohtake T, Motomura W, Takahashi N, Hosoki Y, Miyoshi S, et al. Increased expression of PPAR in high fat diet-induced liver steatosis in mice. Biochem Biophys Res Commun 2005;336:215–22.
[27] Ip E, Farrell GC, Robertson G, Hall P, Kirsch R, Leclercq I. Central role of PPARα-dependent hepatic lipid turnover in dietary steatohepatitis in mice. Hepatology 2003;38:123–32.
[28] Ishii M, Iizuka K, Miller BC, Uyeda K. Carbohydrate response element binding protein directly promotes lipogenic enzyme gene transcription. Proc Natl Acad Sci USA 2004;14:2819–30.
[29] Lopez JM, Bennet MK, Sanchez HB, Rosenfeld JM, Osborne TF. Sterol regulation of acetyl coenzyme A carboxylase: a mechanism for coordinate control of cellular lipid. Proc Natl Acad Sci USA 1996;93:1049–53.
[30] Phillips C, Owens D, Collins P, Tomkin GH. Microsomal triglyceride transfer protein: does insulin resistance play a role in the regulation of chylomicron assembly? Atherosclerosis 2002;160:355–60.
[31] Mirandola S, Realdon S, Iqbal J, Gerotto M, Dal Pero F, Bortoletto G, et al. Liver microsomal triglyceride transfer protein is involved in hepatitis C liver steatosis. Gastroenterology 2006;130:1661–9.
[32] Letteron P, Sutton A, Mansouri A, Fromenty B, Pessayre D. Inhibition of microsomal triglyceride transfer protein: another mechanism for drug-induced steatosis in mice. Hepatology 2003;38:133–40.
[33] Sliskovic I, Raturi A, Mutus B. Characterization of the S-Denitrosation activity of protein disulfide isomerase. J Biol Chem 2005;280(10):8733–41.
[34] Hussain MM, Bakillah A, Jamil H. Apolipoprotein B binding to microsomal triglyceride transfer protein decreases with increases in length and lipidation: implications in lipoprotein biosynthesis. Biochemistry 1997;36:13060–7.
[35] Bakillah A, Hussain MM. Binding of microsomal triglyceride transfer protein to lipids results in increased affinity for apolipoprotein B: evidence for stable microsomal MTP/lipid complex. J Biol Chem 2001;276:31466–73.
[36] Bakillah A, Nayak N, Saxena U, Medford RM, Hussain MM. Decreased secretion of apoB follows inhibition of apoB-MTP binding by a novel antagonist. Biochemistry 2000;39:4892–9.